Scientia Iranica A (2014) 21(4), 1281–1296

Sharif University of Technology
Scientia Iranica
Transactions A: Civil Engineering
www.scientiairanica.com

Influence of fines content and type on the small-strain shear modulus of sand

N. Akbari Paydar and M.M. Ahmadi*

Geotechnical Engineering Group, Department of Civil Engineering, Sharif University of Technology, Tehran, Iran.

Received 25 February 2013; received in revised form 28 August 2013; accepted 17 November 2013

KEYWORDS
Small-strain shear modulus;
Sand;
Fines content;
Plastic fines;
Non-plastic fines.

Abstract. The small-strain shear modulus, G_0, is an important fundamental soil property. Although many studies have been conducted on this property for clean sands and pure clays, small-strain behavior for mixtures of sand and fines has been less addressed. This paper presents the results of a comprehensive laboratory study on G_0 value of sand containing various amounts of different fines. To this aim, bender elements were integrated into a conventional triaxial apparatus, and shear wave velocity was measured on samples of sand with different amounts of highly-plastic, medium-plastic, low-plastic, or non-plastic fines at different void ratios. Measuring the shear wave velocity and thus obtaining G_0 at different void ratios and effective stresses, the intrinsic parameters that characterize G_0 were determined for the tested materials. This allowed the effects of fines type and content on the G_0 value of sand to be evaluated in a systematic manner. The G_0 values of different sand-fines mixtures were compared based on different density parameters. Results show that G_0 of silty and clayey sands is affected by both fines content and fines type. Therefore, in order to estimate G_0 of sand-fines mixture, not only the fines content but also their plasticity needs to be properly accounted.

1. Introduction

The small-strain, initial, or maximum shear modulus of soil (G_0) is an important fundamental property in geotechnical engineering. It is a key parameter in all small-strain practical geotechnical problems, especially earthquake engineering, the study of the actions of wind, design of machine foundations, and soil-structure interaction. This parameter is also used to evaluate the liquefaction resistance of soils.

The stress-strain response of soil is highly nonlinear, and soil stiffness (G) degrades with increase in the shear strain magnitude (Figure 1). However, the small-strain shear modulus is defined within the initial linear elastic portion of the stress-strain curve at very small-strain range and is, therefore, relatively independent of strain level.

Under the assumption of soil as an elastic medium at very small strains, G_0 can be determined from shear wave velocity, according to the theory of elasticity, using the equation:

$$G_0 = \rho V_s^2, \tag{1}$$

where ρ and V_s are the density and shear wave velocity, respectively.

In view of the above, G_0 can be readily calculated from the laboratory measurements of the shear wave velocity, for which bender elements and resonant column tests are often used. Bender element testing [1] has become a standard procedure for the determination of the small-strain shear modulus. The test is nondestructive and has been used extensively on laboratory

*. *Corresponding author. Fax: +98 21 66014828*
E-mail address: mmahmadi@sharif.edu (M.M. Ahmadi)

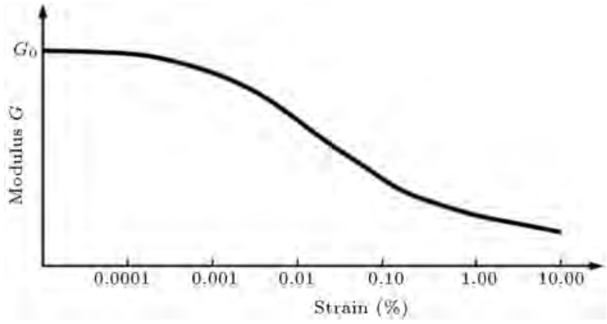

Figure 1. Variation of shear modulus (G) with strain amplitude.

samples [2] owing to its reliability for G_0 calculation. The maximum shear strain induced by bender elements is measured to be less than 10^{-5}, falling in the range of very small strains [2].

The small-strain shear modulus of clean sands has been extensively studied so far [3-10]. Besides, a large number of studies have been undertaken on small-strain shear modulus of pure clays [11-19]; nevertheless, small-strain behavior of sand-fines mixtures has been less studied. In other words, natural sands usually contain fine particles whose effects on G_0 are inadequately addressed so far [20]. Lack of this kind of study is more evident for clayey sands compared to silty sands.

The most important studies on the effects of non-plastic fines on the small-strain shear modulus of sands are as follows.

Resonant column tests performed by Iwasaki and Tatsuoka showed that for a constant void ratio, G_0 decreases rapidly with increase in non-plastic fines content up to 14% [21]. Significant reduction in G_0 with the addition of non-plastic fines was also considered for the estimation of the axial capacity of driven piles by Randolph et al. [22]. They proposed that at a constant void ratio, the small-strain stiffness of silty sand with the range of fines content (smaller than 0.2 mm) of 5-10, 10-15, and 15-30% is as lower as about 50, 25, and 19% of the G_0 value of sand containing less than 5% fines, respectively. Salgado et al. performed a series of bender element tests on samples of Ottawa sand with fines content in the range of 5-20% [23]. They showed that G_0 decreases dramatically with the addition of even small percentages of silt. For example, they reported 16, 26, 48 and 53% of G_0 reduction for sands with 5, 10, 15 and 20% fines, respectively, compared to clean sand at a confining pressure of 100 kPa and relative density of 50% [23]. Reduction in the magnitude of the shear wave velocity with increasing non-plastic fines of sand up to 30% has also been observed in the tests performed by Huang et al. [24].

However, much fewer studies have been performed on the effects of plastic fines and their plasticity on the small-strain shear modulus of sands. There are also inconsistencies in the results of the undertaken studies.

Previous studies showed that for normally consolidated clayey soils, G_0 does not depend on the plasticity of the fines, but it increases with plasticity for 5over-consolidated soils [25]. Whereas, Zen et al. reported that G_0 increases with increasing Plasticity Index (PI) for Toyoura sand mixed with marine clay [26]. Later tests by Wang and Kuwano on mixtures of Toyoura sand with natural marine clay in constant void ratio approved the previous findings on the increase of G_0 with plastic fines [27]. Recently, Carraro et al. performed a total number of about 300 bender element tests on two sets of mixtures of Ottawa sand with 2, 5, 10, and 15% of non-plastic silt and 2, 5 and 10% of Kaolin clay, and voted for the reduction of G_0 with increasing the fines content for both plastic and non-plastic fines [28]. They showed that the small-strain response of sands containing either plastic or non-plastic fines is affected by the plasticity of the fines added to the host sand, and so G_0 is affected by both the amount of fines and their nature. They stated that the small-strain stiffness of clayey sands is typically higher than that of sands containing non-plastic silt at similar relative densities and stress states. Nevertheless, only one type of low-plastic clay (PI = 26%) was used in their research; therefore, detailed examination of the effects of the fines plasticity on the small-strain shear modulus was not considered.

In summary, the limited research on the effects of low percentages of non-plastic fines on small-strain shear modulus of sands indicates the reduction of G_0 with increasing the fines content. However, further investigation is needed about the effects of high percentages of non-plastic fines on G_0. Also few studies have been conducted on the effects of the plastic fines and their plasticity on G_0 of sands and the presented results, according to different fines used in the different studies, are conflicting. Therefore, the main objective of this study is to contribute to a better understanding of the influence of the amount of fines and their plasticity on the small-strain shear modulus of sand-fines mixtures at different densities and effective stresses. For this purpose, more than 2100 bender elements tests were carried out on 188 saturated samples of sand mixed with different fines types and content.

2. Empirical relations for G_0

The small-strain shear modulus for granular soils is mainly a function of void ratio and effective confining stress. A comprehensive series of resonant column tests were performed by Hardin and Richart to obtain the G_0 for Ottawa sand and crushed quartz sand [3]. They proposed the following empirical relations for G_0 at a shear strain of 10^{-4} or less:

$$G_0 = C_g P_A^{1-n_g} \frac{(e_g - e)^2}{1+e} {\sigma'}_m^{n_g}, \tag{2}$$

where P_A is a reference stress being equal to atmospheric pressure, e_g, n_g and C_g are intrinsic parameters depending solely on the soil type, and σ'_m is the mean effective stress in the same units as the reference stress given by:

$$\sigma'_m = \frac{1+2k_0}{3}\sigma'_v. \tag{3}$$

Here, σ'_v is the vertical effective stress, and K_0 is the ratio of effective horizontal stress to effective vertical stress.

Salgado et al. found that Eq. (2) works well for both clean and silty sand [23]. The same observation was made by Carraro et al. for sands containing low plastic fines up to 10% [28].

A different form of the Hardin and Richart [3] G_0 equation has been proposed by Jamiolkowski et al. [29] as:

$$G_0 = C_g P_A^{1-n_g} e^{a_g} {\sigma'}_m^{n_g}, \tag{4}$$

where a_g, n_g and C_g are intrinsic parameters associated with soil type, similar to Eq. (2). Salgado et al. showed that Eq. (4) works even better than Eq. (2) for silty sand with silt contents up to 15% [23].

3. Tested materials

In the present study, standard Firoozkooh No. 161 sand was used as the host sand. This sand is of crushed silica type with angular grains which is commercially available from Firoozkooh mine in the northeast of Tehran city. This sand is commonly used as the standard sand in geotechnical testing in Iran. The fine part of the tested soils consisted of three types: Firoozkooh micronized powder from the same mine of the host sand as the non-plastic fine (silt), Kaolin clay as the low-plastic fine, Bentonite clay as the highly-plastic fine and a mixture of Bentonite and Kaolin clay as the medium-plastic fine. The physical properties of these materials are summarized, in Table 1, together with the corresponding grain size distribution curves in Figure 2.

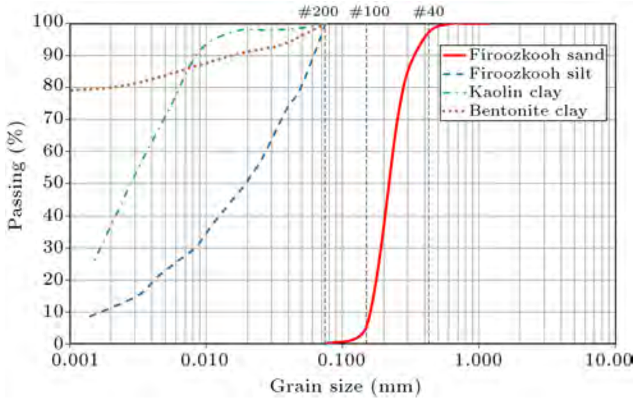

Figure 2. Grain size distribution curves of the mixtures constituents

Soil specimens of sand with non-plastic fines contents of 0, 3, 5, 15, 25, 35, 50, 75 and 100% and plastic fines contents of 5 and 15% were considered in this study. The Fines Content (FC) is defined as the ratio of the dry weight of the fines to the total dry weight of the mixture.

4. Specimen preparation, testing device and procedure

4.1. Testing device

In bender element tests, the element which is used as the transmitting bender is located at one end of the sample, which causes shear waves due to vibrations resulting from voltage change. These waves bring about a maximum shear strain of less than 10^{-5} and vibrate the receiving bender at the other side of the sample. The shear wave velocity is obtained by dividing the sample length (L) to the measured travel time between the two elements (t) as:

$$V_s = L/t. \tag{5}$$

In the current study, the bender elements were installed in a conventional triaxial apparatus at the top and the bottom pedestal of the triaxial cell. The initial embedded lengths of the bender elements into the sample were 6 mm. A diagram of the triaxial system equipped with bender elements is shown schematically

Table 1. Physical properties of the tested materials.

Material	Unified soil classification	D_{50}	C_u	LL	PI	G_s
Firoozkooh sand	SP	0.23	1.32	-	-	2.653
Firoozkooh silt	ML	0.02	-	26	2	2.659
Kaolin clay	CL	0.003	-	43	18	2.690
Bentonite clay	CH	-	-	160	116	2.752

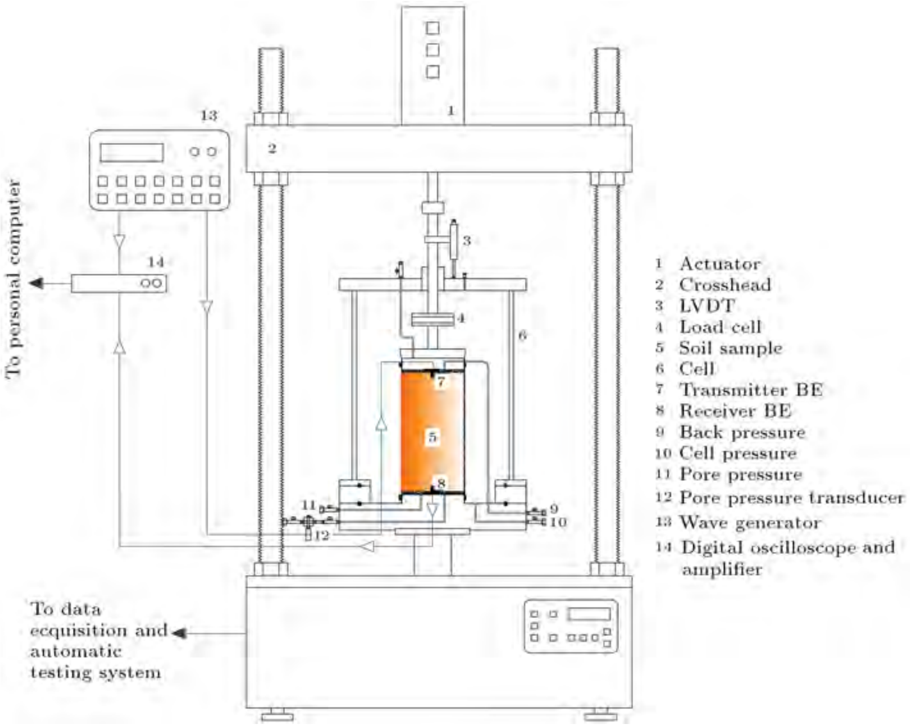

Figure 3. Schematic diagram of the triaxial system equipped with bender elements.

Figure 4. Installed bender elements at top cap as transmitting bender (left) and bottom pedestal as receiving bender (right).

in Figure 3. Also installed bender elements at the top cap and the bottom pedestal, respectively, as transmitting and receiving benders are shown in Figure 4.

4.2. Specimen preparation

In view of the diversity of the specimen reconstitution techniques (e.g. dry or water pluviation, moist tamping, slurry deposition, etc.), obtaining homogeneous samples in terms of void ratio distribution and consistency as well as covering a wide range of void ratios are the basic requirements. Huang et al. showed that the specimens prepared by moist tamping are reasonably uniform and give sufficiently repeatable V_s values [24]; moreover, it gives the widest range in void ratio among others [30]. Therefore, moist tamping method of sample reconstitution was utilized to prepare the samples in the present study. Samples with different initial void ratios were prepared for each tested mixture.

The specimens were 70 mm in diameter and 140 mm in height. For the mixtures, sand and fine materials were first dried in the oven prior to mixing together and then 5% of water was added to the mixture. The specimens were compacted to the desired density in seven layers, each of 20 mm thick in a cylindrical split mold. In order to achieve uniformity in density throughout the sample height, the under-compaction method proposed by Ladd [31] was used. The under-compaction method consists of placing each layer at a density slightly greater than the density of the layer below. Owing to the fact that compaction of each succeeding layer further densifies the underlying lower layers, the compaction density of each layer was varied linearly from the bottom to the top, with the bottom (first) layer having the lowest density. For this purpose, the relative density was varied by 1% per layer so that the intermediate layer has the target density. Using the above method, according to the desired density of the each layer, the weight of wet soil was identified and compacted carefully with an aluminum tamper consisting of a circular disk. After compaction of each layer and leveling and scraping top of the layer, the next layer was poured and compacted with the same procedure. Before the split mold was disassembled, a partial vacuum of 10 to 20 kPa was applied to form the specimen to reduce disturbance during the removal of mould and triaxial cell installation. Next, the mold was dismantled and after measuring the initial specimen height and diameter, the triaxial cell was assembled around the sample and filled with water.

4.3. Testing procedure

All bender element tests in this study were performed on saturated samples. To facilitate the saturation process, at an effective stress of less than 20 kPa, carbon dioxide (CO_2) was first passed through the samples for at least 30 minutes. Subsequently, de-aired water was allowed to flow into the specimens from the bottom valve to the top valve exposed to atmosphere. Samples were then subjected to increments in the confining stress while monitoring the associated rise in pore pressure and saturated by applying proper incrementally back pressure in successive steps. The Skempton pore pressure parameter (i.e. B value which is defined as the ratio of the increase in excess pore water pressure resulting from an increase in confining pressure) was determined as the indicator of the degree of saturation. Samples were considered to be fully saturated if B value was greater than 0.95. Any samples that did not have a B value of at least 0.95 were discarded. As previous researchers have also demonstrated [32], the saturation process in samples with a high percentage of fines took a considerable amount of time.

Saturated samples were then consistently consolidated uniformly in steps of 10 to 30 kPa. At each step of consolidation, depending on the type of materials, sufficient time from several minutes to several hours was given to complete each the consolidation step. The consolidation process continued until the effective confining stress reached a value of 200 kPa. Immediately after the end of each consolidation step (ranging from 30 to 200 kPa), the shear wave velocity was measured using bender elements.

In all the conducted bender element tests, a single sinusoidal pulse having a frequency of 5 kHz and amplitude of ± 10 Volts was used as the transmitted signal. The value of L in Eq. (5) is assumed the tip-to-tip distance of the bender elements [33]. In order to obtain the travel time from the source to the receiver, t in Eq. (5), the method of first arrival time was used. First arrival time refers to the time interval between the start of the source signal and the start of the major cycle of the received signal by ignoring the initial portion of the weak signal. This weak signal indicates the presence of the near field effect and should be eliminated [33,34]. Sample result of a bender element test on a sample of sand containing 5% of Kaolin with a void ratio of 0.720 at an effective confinement stress of 80 kPa is represented in Figure 5 in which the first arrival time is shown.

The void ratio as well as the height of the samples changes in each consolidation step as the confinement stress increases. To calculate the changes in the void ratio, the amount of water expelled from the specimen during consolidation steps was measured, using a sensitive volume change apparatus. Also,

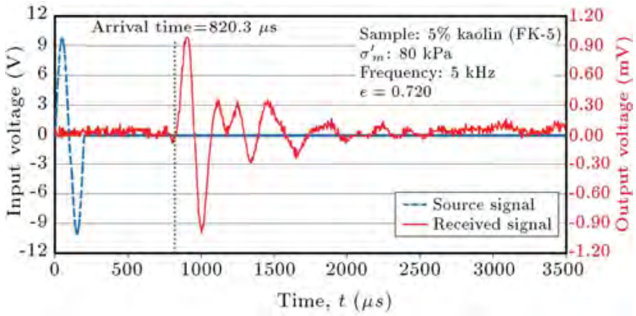

Figure 5. Representative result of bender element tests.

the water content of the entire sample was measured carefully at the end of the experiment. To measure the water content of the sample at the end of the experiment, at first step, the bottom valve of the sample was opened and a confining stress of approximately 50 kPa was applied. The free water weight, expelled from the sandy sample, was accurately measured. At second step, the entire moist sample was carefully taken out of the apparatus and its moisture content was also measured. The water content of the sample is the sum of the free water measured in the first step and the moist content measured in the second step. Given that the sample is already saturated prior to the consolidation phase, the void ratios at the earlier stages of consolidation can be back-calculated from these measured values. The change in height of the sample was also measured during the saturation and consolidation phases using two displacement transducers, and was accordingly used in calculating the shear wave velocity using Eq. (5). An example of the results obtained for a single sample of sand containing 3% of non-plastic fines is presented in Figure 6. Thus, from the bender element tests performed on a certain sample, at different void ratios and confinement effective stresses at successive steps of consolidation phase, the shear wave velocity is conveniently achieved.

Following the above procedure, more than 2100 bender elements tests on 188 different samples were performed for which the corresponding shear wave velocities were obtained for each combination of the tested sand-fines mixtures under different void ratios and confinement effective stresses (Table 2).

As it is clear from Table 2, the accessible range of void ratios is narrower for higher fines content, so lower densities were not achievable for sand mixtures containing higher percentages of fines. This is due to the occurrence of significant volume contraction during the saturation stage of specimen preparation, as reported by Sladen and Handford [35], Pitman et al. [36], Yamamuro and Covert [37], Huang et al. [24] and Derakhshandi et al. [38]. This effect cannot be avoided when reconstituting sand specimens with fines [38].

Point no#	Void ratio (e)	Sample height (mm)
1	0.68	137.71
2	0.674	137.69
3	0.673	137.63
4	0.672	137.61
5	0.671	137.58
6	0.670	137.56
7	0.670	137.54
8	0.669	137.50
9	0.669	137.49
10	0.668	137.48
11	0.668	137.46
12	0.667	137.45
13	0.667	137.43
14	0.666	137.42
15	0.666	137.40
16	0.665	137.39
17	0.665	137.36

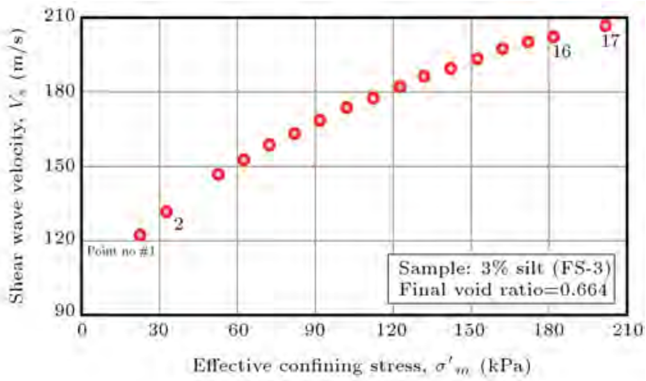

Figure 6. An example of shear wave velocity measurement at the different steps of consolidation for a single sample.

Table 2. Number of samples and tests performed on various combinations of sand and fines and range of void ratios.

Material identification code	Fines content (%)			No. of samples	No. of bender elements tests	Range of void ratios for tests	
	Silt	Kaolin	Bentonite			Min	Max
F0-0	0	0	0	25	228	0.67	0.89
FS-3	3	0	0	14	193	0.66	0.86
FS-5	5	0	0	21	235	0.65	0.89
FS-15	15	0	0	17	191	0.53	0.77
FS-25	25	0	0	21	220	0.47	0.69
FS-35	35	0	0	9	90	0.40	0.53
FS-50	50	0	0	4	55	0.38	0.47
FS-75	75	0	0	5	73	0.47	0.57
SS-100	100	0	0	4	56	0.66	0.80
FK-5	0	5	0	17	213	0.64	0.80
FK-15	0	15	0	13	168	0.50	0.70
FB-5	0	0	5	10	145	0.66	0.82
FB-15	0	0	15	7	40	0.61	0.77
FK50B50-15	0	7.5	7.5	10	100	0.57	0.72
FK30B70-15	0	4.5	10.5	11	119	0.57	0.73

4.4. Scanning electron microscopy

To evaluate how the fine and the coarse particles are placed next to each other for various mixtures of sand and fines with different densities and to study their fabric, Scanning Electron Microscope (SEM) imaging was used. For this purpose, the samples were first reconstituted using the wet tamping method under two different densities: dense and loose, which were subsequently used for imaging after being dried in the oven.

5. Experimental results and analysis

5.1. Intrinsic parameters of G_0

Having computed the G_0 value of the tested materials from measured shear wave velocity at different stresses and void ratios, the effect of fines type and content on the small-strain shear modulus of sand can be investigated. To illustrate the matter quantitatively, the empirical relations (Eqs. (2) and (4)) described in Section 2 can be used. The intrinsic parameters of these equations were determined by fitting the results of the bender element tests conducted at different consolidation stresses and void ratios for each of the tested materials (Table 3). Table 3 shows that the values of correlation coefficient, R^2, for all combinations are very close to 1.0. The calculated G_0 values obtained by using Eqs. (2) and (4) against the measured G_0 values are shown in Figures 7 and 8, respectively. These figures as well as the values of correlation coefficient, R^2, illustrate the high accuracy of these correlation equations (Eqs. (2) and (4)) in estimating G_0 from

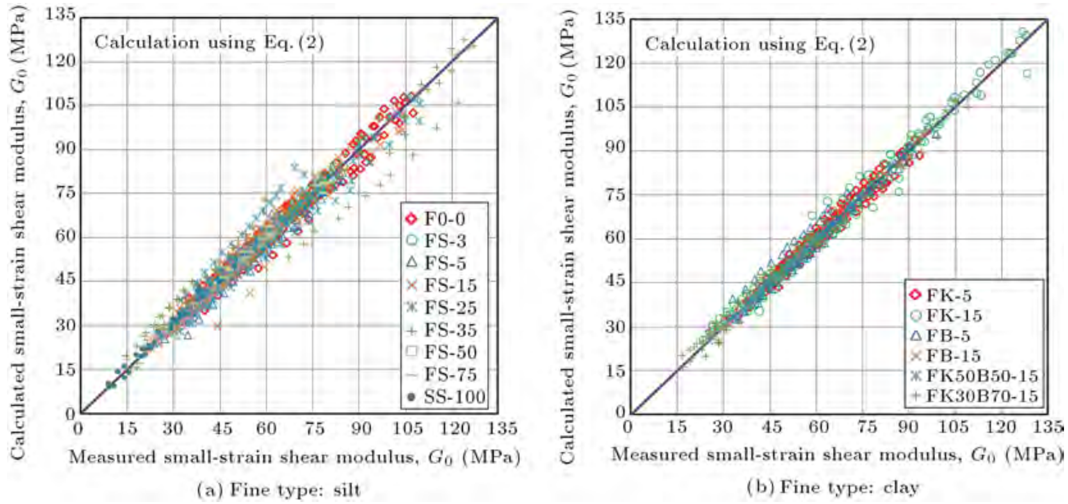

Figure 7. Calculated G_0 values by Eq. (2) against measured values for a) sand-silt mixtures, and b) sand-clay mixtures.

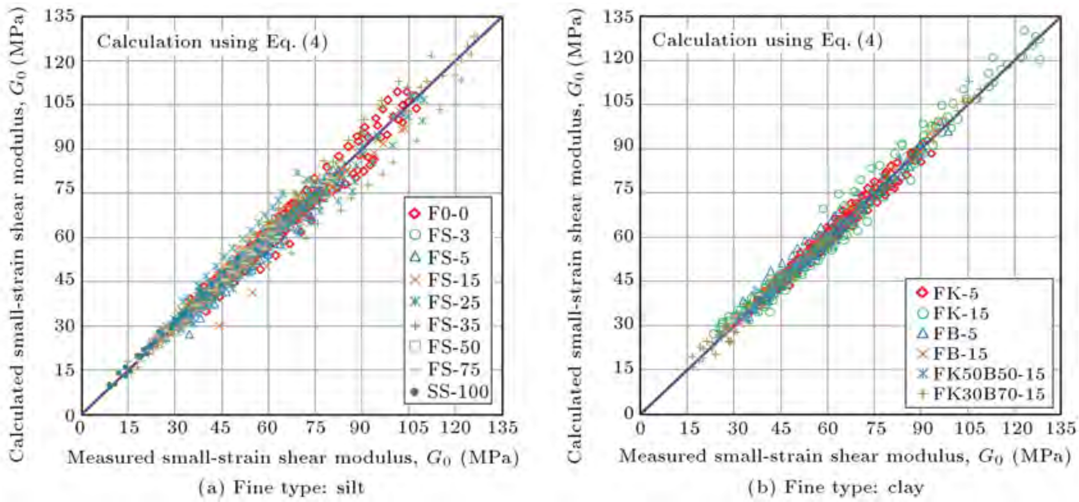

Figure 8. Calculated G_0 values by Eq. (4) against measured values for a) sand-silt mixtures, and b) sand-clay mixtures.

Table 3. Fitted intrinsic parameters for Eqs. (2) and (4) to evaluate the small-strain shear modulus of the tested materials.

Material	Intrinsic parameters for Eq. (2)				Intrinsic parameters for Eq. (4)			
	C_g	n_g	e_g	R^2	C_g	n_g	a_g	R^2
F0-0	772	0.48	1.97	0.96	389	0.48	-1.84	0.95
FS-3	110	0.50	3.66	0.99	404	0.50	-0.94	0.99
FS-5	123	0.50	3.46	0.97	380	0.49	-1.05	0.97
FS-15	758	0.52	1.68	0.95	249	0.51	-1.55	0.96
FS-25	2334	0.50	1.16	0.93	150	0.51	-2.14	0.94
FS-35	6500	0.48	0.82	0.93	22	0.48	-4.04	0.94
FS-50	100	0.65	2.80	0.99	235	0.68	-0.60	0.99
FS-75	449	0.60	1.78	0.99	155	0.54	-1.68	0.99
SS-100	100	0.66	3.13	0.99	228	0.60	-1.18	0.99
FK-5	447	0.49	2.16	0.98	335	0.48	-1.41	0.97
FK-15	4787	0.36	1.04	0.98	115	0.36	-3.10	0.97
FB-5	1474	0.45	1.56	0.97	290	0.46	-2.18	0.97
FB-15	2639	0.41	1.28	0.99	197	0.43	-2.70	0.99
FK50B50-15	4310	0.39	1.08	0.99	117	0.41	-3.29	0.99
FK30B70-15	6500	0.39	1.02	0.99	85	0.38	-4.17	0.99

void ratio and effective stress for clean sand, silty sand, sandy silt, and clayey sand.

Obtained n_g, which is indicative of the effect of the confinement stress on G_0, is approximately the same, using either Eq. (2) or Eq. (4). The G_0 curves resulting from Eqs. (2) and (4) versus void ratio for different combinations of fines and sand for an isotropic effective stress of 100 kPa are compared in Figure 9, in which the corresponding intrinsic parameters from Table 3 are used. Obviously, similar curves can be drawn for any arbitrary mean effective stresses ranging from 30 to 200 kPa (i.e. test range). As there is no significant difference between R^2 for Eqs. (2) and (4) and therefore the accuracy of these equations for the tested sand mixtures is similar, Eq. (4) was selected to evaluate the results in the following.

5.2. *The effect of fines content on G_0*

To evaluate the effect of fines on the mechanical behavior of sand-fines mixture, a decision must be made regarding the density parameter. The density parameters most commonly used are: global void ratio, e, relative density, D_r, inter-granular or skeleton void ratio, e_s, and equivalent granular void ratio, e^*. There is no consensus on the more suitability of one over the others in silty or clayey sands. In this paper, using global void ratio, skeleton void ratio and equivalent granular void ratio, the effect of fines content on G_0 of sand is evaluated considering fines type.

5.2.1. *The effect of fines content on G_0 in terms of void ratio*

The small-strain shear modulus determined for the various combinations of sand and fines were first examined in terms of their void ratios. The G_0 curves versus void ratio at an isotropic consolidation stress of 100 kPa are provided in Figure 9 for the tested soils. Remarkably, for other isotropic effective stresses in the experimental range (i.e. from 30 to 200 kPa), the similar curves and results will be obtained. In other words, the trend of changes for G_0-e curves, corresponding to different fines content, will be similar. For all the tested soils, the well-known decrease of G_0 by increasing the void ratio was observed. It can be seen from Figure 9(a) that the maximum rate in the reduction of shear modulus with increase in the void ratio occurs for silty sand with 35% fines content (FS-35), for which 0.13 void ratio increase (equivalent to less than 5% decrease in density) leads to one-third value of G_0. Figure 9(a) shows that at a constant void ratio, the addition of up to 25% non-plastic fines to sand results in a continuous reduction in G_0. But, as the void ratio ranges of tests are different for tested soils, it is difficult to conclude the same trend for higher fines contents. However, comparing the 25% (FS-25) curve with the 35% (FS-35) curve or comparing the 35% curve with the 50% (FS-50) curve

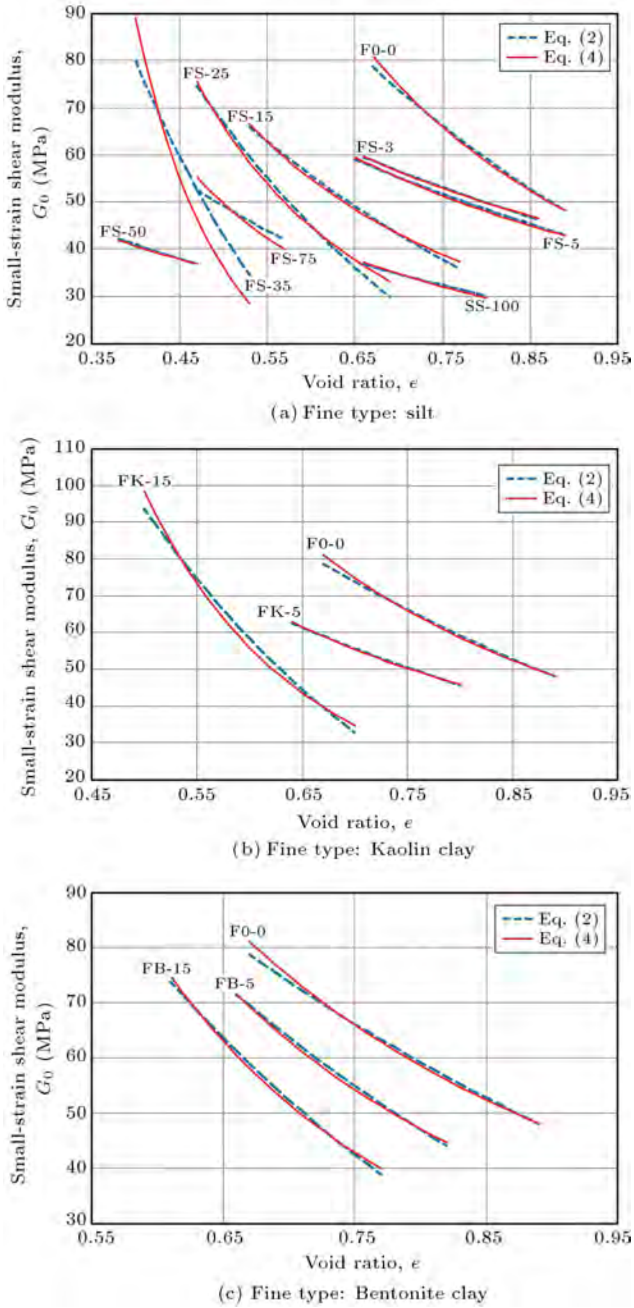

Figure 9. The G_0 curves versus void ratio at an isotropic consolidation stress of 100 kPa for the combination of sand with a) silt, b) Kaolin clay, and c) Bentonite clay.

shows that increasing the fines content from 25% to 35% and also from 35% to 50% will decrease G_0 at a constant void ratio. However, comparing the 50% curve with the 75% (FS-75) curve shows that increasing the fines content from 50% to 75% will increase G_0 slightly at a constant void ratio. Therefore, it is concluded that there is a threshold value for fines content beyond which higher G_0 values are anticipated. According to the obtained results, threshold fines content for the mixtures of tested sand and silt is around 50% in this study. It should be noted that the threshold fines

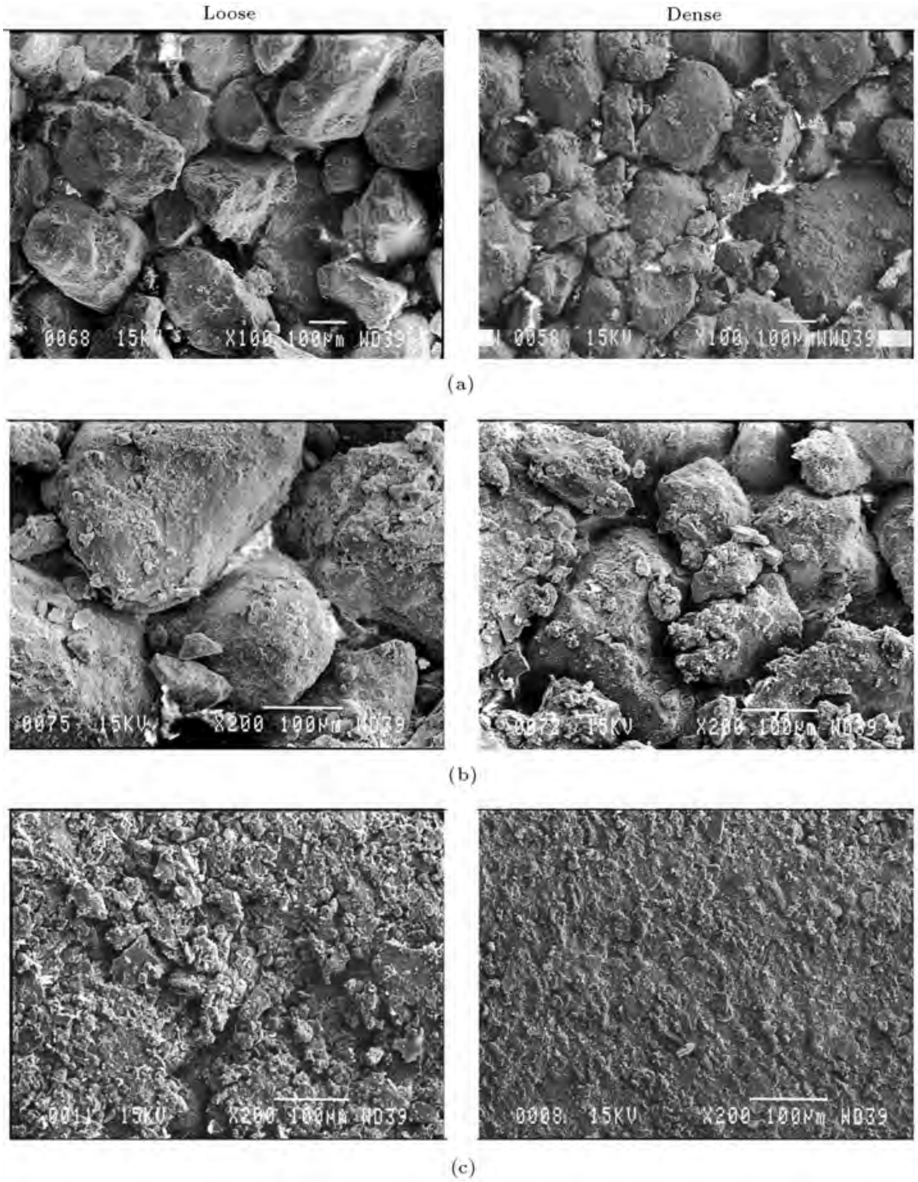

Figure 10. Scanning Electron Microscope (SEM) photographs of sand-silt mixtures with a) 5% silt (FS-5), b) 15% silt (FS-15), and c) 75% silt (FS-75).

content depends on the characteristics of the base sand as well as the fines particles.

Figure 9(a) also shows that adding a small amount of non-plastic fines (e.g. 3% and 5%) to sand at low void ratios (dense state) results in a significant reduction in G_0 value, while this reduction is lower at high void ratios (loose state). This is because at higher void ratios, due to the presence of more spaces between the coarse particles, the non-plastic fine-grained particles are mostly placed in the spaces between sand particles. In this case, the contacts between coarse particles are not substantially affected by adding the fines. As a result, the fines are less involved, and shear waves are basically transmitted through coarse-grained particles. However, at lower void ratios, adding even small amounts of fine particles lead to considerable reduction in G_0 due to weakening the coarse particle contacts by interfering between them.

To further illustrate the above, a series of SEM images were taken from the samples. Figure 10(a) and (b) show the SEM images of sand-silt mixtures at two different densities (i.e. loose and dense) for 5 and 15% of fines content, respectively. It is shown in Figure 10(a) that for a mixture of 5% silt with sand, at the loose state, the fines are not observed in the image, where for the dense state, the fines are vividly present. This means that for 5% silt content at the loose state, the fines fill up the voids between the grains, and do not necessarily affect the coarse grain contacts. However, in the dense state, as it is shown in Figure 10(a), the fines can affect the coarse grains contacts result in a larger

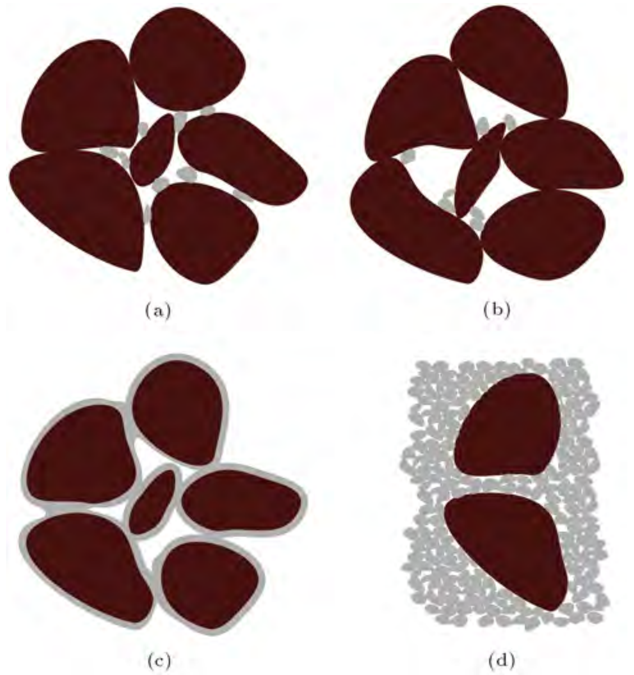

Figure 11. Schematic representation of particle arrangement: a) sand-silt mixture with low void ratio; b) sand-silt mixture with high void ratio; c) sand-clay mixture and d) sand-silt mixture with high percentage of non-plastic fines.

reduction of the shear wave velocity and consequently the G_0 value due to weak developed contacts between fine and coarse particles. Comparing Figure 10(a) and (b) indicates that for the mixture of 15% silt and sand, even at the loose state, the coarse grains contacts are affected by the presence of fines. Arrangements of coarse and fine particles are shown schematically in Figure 11. Figure 11(a) represents the combination of sand with a high percentage of non-plastic fines (lower than the threshold fines content) or sand-silt mixture with low void ratio. Here, the fabrics of the soil can be considered floating as in an idealized two-sized particle packing introduced by Thevanayagam et al. [39], since coarse particles have the lowest contact with each other and they are surrounded by the fine particles. This is while the combination of sand with low percentage of non-plastic fines or sand-silt mixture with high void ratio has non-floating fabrics. This fabric (i.e. non-floating fabric) is illustrated schematically in Figure 11(b). In non-floating fabrics, soil behavior is mostly controlled by the coarser particles [39]. Note that, increasing the fines content at constant void ratio changes the soil fabric from non-floating to floating and hence G_0 decreases. This explanation is in agreement with Salgado et al. [23].

The addition of highly-plastic fines, i.e. Bentonite clay, to sand at constant void ratio lowers the G_0 value similar to non-plastic fines (Figure 9(c)). Based on this figure, unlike the non-plastic fines, the rate of G_0 reduction because of adding highly-plastic fines to sand is almost constant at different void ratios. This is because of the very small size of the plastic fine particles and their high cohesion resulting in a fine layer surrounding the coarse particles even at high void ratios, as illustrated in Figure 11(c). It is evident from the SEM images in Figure 12 that for sand with plastic fines, even at low percentages of fines, coarse particles are surrounded by fine particles, contrary to sand with non-plastic fines which this happens only with increasing the fines content. Therefore, for different void ratios, the fine particles are involved in shear wave transmission in both dense and loose states, and the small-strain shear modulus is reduced with the addition of the plastic fines.

The small-strain behavior of sand with low-plastic fines (Kaolin clay) in Figure 9(b) shows an intermediate behavior between sand with non-plastic fines and sand with highly-plastic fines.

At high percentages of non-plastic fines content (i.e. sandy silt) above 50%, coarse particles are completely floated within fine particles. This may be observed in the schematic arrangements of coarse and fine particles in Figure 11(d) and also in the SEM images for 75% non-plastic fines content in Figure 10(c). Therefore, fine particles play a major role in the transmission of shear waves. As a result, G_0 values increases slightly with increase in the fines content from 50 to 100% due to relatively better developed contacts between non-plastic fine particles than between fine and coarse particles. However, this increase is negligible, so that in a given void ratio, the G_0 value for pure sand is about two times the G_0 value for silt.

5.2.2. The effect of fines content on G_0 in terms of skeleton void ratio

To assess the effect of fines content on G_0, inter-granular or skeleton void ratio, e_s, could be used instead of global void ratio, e. The global void ratio of the soil is defined as the ratio of the volume of voids to the volume of solids, while the inter-granular or skeleton void ratios consider the volume occupied by the fine particles, as if it were void space. In other words, it is assumed that fines simply occupy the voids in the sand skeleton and the behavior is controlled by sand skeleton only. Therefore, the definition of skeleton void ratio by assuming that fines are completely non-active is not universally applicable for the entire range of fines content [40]. Georgiannou et al. [41] and Thevanayagam [42] showed that skeleton void ratio may only be an adequate concept for low fines content. This parameter is not a suitable density parameter for silty sands with high percentages of fines.

When the specific gravities of solids (G_s) for the coarser and the finer fractions of the soil are the same,

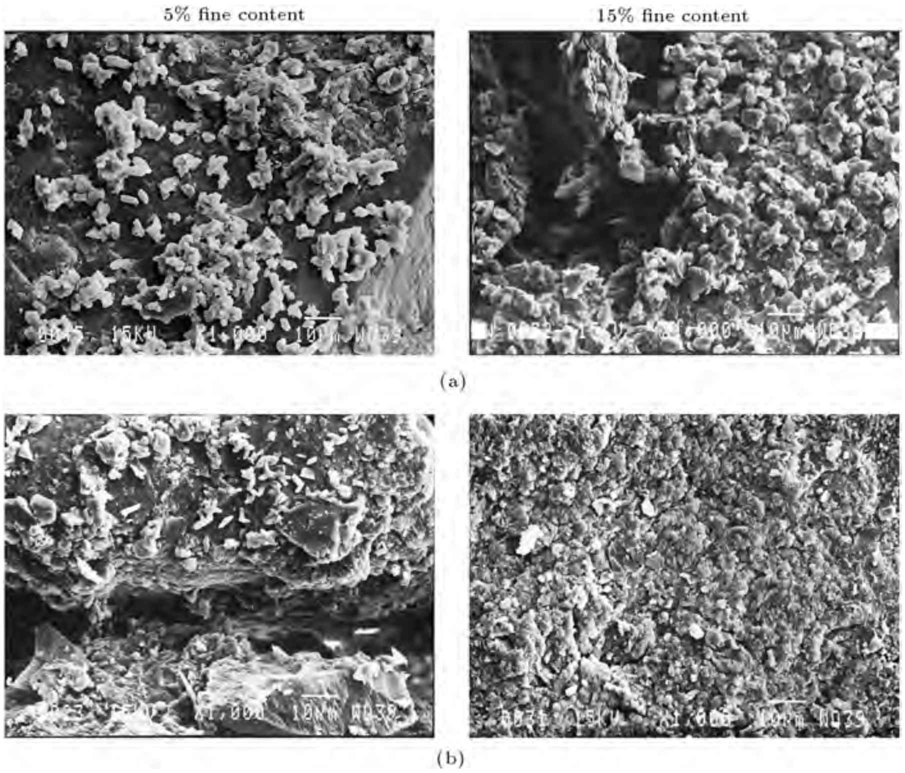

Figure 12. Scanning Electron Microscope (SEM) photographs of sand-clay mixtures: a) Kaolin clay; and b) Bentonite clay.

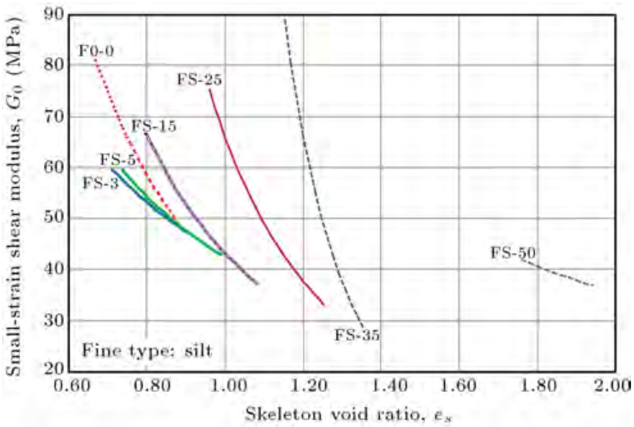

Figure 13. The G_0 curves versus skeleton void ratio at an isotropic consolidation stress of 100 kPa for the combination of sand with silt.

the skeleton void ratio (e_s) is defined as:

$$e_s = \frac{e + \mathrm{FC}}{1 - \mathrm{FC}}, \tag{6}$$

where FC is ratio of dry weight of fines to the total dry weight of solids.

The curves of G_0 against skeleton void ratio (e_s) at an isotropic consolidation stress of 100 kPa are plotted in Figure 13 for combinations of sand with less than 50% silt. For low skeleton void ratio, by adding a small amount of non-plastic fines, the small-strain shear modulus first decreases slightly which then increases by further adding fines (Figure 13). For low percentages of non-plastic fines (i.e. FC$\leq$15%) at high sand skeleton void ratios, the G_0-e_s curves become close, because the fines mostly fill the void space and have no affect on the shear wave transmission. Further increase in the amount of fines for constant skeleton void ratio improves the contacts between fine particles so that the G_0 value increases. Briefly, according to Figure 13, it can be concluded that if skeleton void ratio is to be considered as density parameter, at a constant skeleton void ratio, G_0 does not change much for silty sand with less than 15% of fines content, especially at high skeleton void ratios.

Owing to the difference in the performance of non-plastic and plastic fines in sand mixtures, the skeleton void ratio is not appropriate for characterizing sand-clay mixtures. In other words, while filling the pore space and then the contacts between coarse grains happen subsequent to each other for silty fines, accumulation of clayey particles around the contact points occurs from the outset of fines addition.

5.2.3. The effect of fines content on G_0 in terms of equivalent granular void ratio

As mentioned in previous section, inter-granular void ratio may be an adequate concept for only low fines content [41,42]. With an increase in fines content, fines may come in between the contact of sand grains and participate in the force structure. Fines that are between coarse particles are in the force chain, whereas fines that are located in the gaps between the coarse grains contribute little to the force structure [40]. A more general concept is to have a fraction of the fines actively participating in the force structure [40]. Thevanayagam [43] introduced the concept of equivalent granular void ratio or inter-granular contact index void ratio (e^*). This approach requires an additional "b" parameter and is defined as:

$$e^* = \frac{e + (1-b)\mathrm{FC}}{1-(1-b)\mathrm{FC}}. \tag{7}$$

In this equation, the physical meaning of b is the fraction of fines that actively participates in the force structure. When $b = 0$, this equation reduces to Eq. (6).

The prediction of the b value, and thus the determination of equivalent granular void ratio, is problematic and controversial [40]. Different researchers have proposed a variety of recommendations to obtain b parameter [44-46]. Recently, Rahman et al. [40] proposed a method to predict b parameter using a semi-empirical approach, based on three input parameters including size ratio of fines and coarse particles, fines content, and threshold fines content [40]. In this study, the b parameter and thus equivalent granular void ratio have been calculated using this method. The curves of G_0 against equivalent granular void ratio (e^*) at an isotropic consolidation stress of 100 kPa are plotted in Figure 14 for combinations of sand with less than 50% silt. In this figure, the values of b parameter are also provided for different fines content. It is worth noting that threshold fines content is assumed to be 50% in calculation of the b parameter. Remarkably, by changing threshold fines content from 35% to 50%, the obtained curves in Figure 14 will not change much.

As seen in Figure 14, the trend of changes is characterized up to 25%. These changes are in such a way that the small-strain shear modulus first decreases slightly which then increases by further adding fines. Also, at high equivalent granular void ratios, the G_0-e^* curves become close. In summary, if the equivalent granular void ratio is to be considered as a density parameter, at a constant e^*, G_0 does not change much, especially at high equivalent granular void ratios for silty sand with less than 15% of fines content (similar to the case of using e_s as density parameter). As the values of b parameter is low for FC = 3% and FC = 5%, e_s and e^* are almost equal for these low fines content and therefore, corresponding curves (i.e. FS-3 and FS-5) in Figures 13 and 14 are almost the same. However, in the case of using e^*, the 15% (FS-15) curves are slightly closer to curves of the smaller fines contents than the case e_s is used. It can also be concluded that similar to e_s, e^* is not applicable for high percentage of fines content.

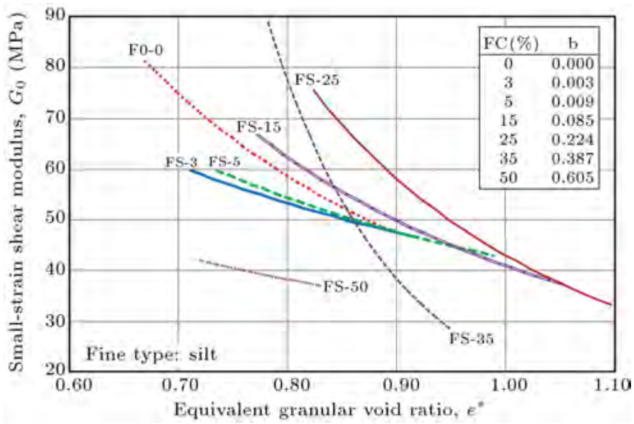

Figure 14. The G_0 curves versus equivalent granular void ratio at an isotropic consolidation stress of 100 kPa for the combination of sand with silt.

5.3. *The effect of fines type on G_0*

The G_0 curves versus void ratio for 5 and 15% fines content at an effective stress of 100 kPa are illustrated in Figure 15(a) and (b), respectively. According to this figure, it can be seen that G_0 depends on the fine

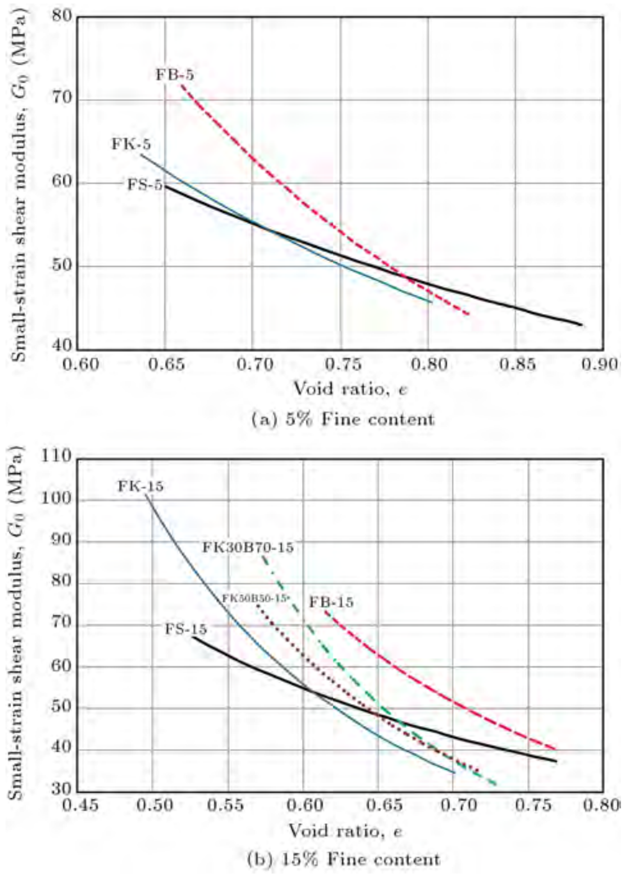

Figure 15. The G_0 curves versus void ratio at an isotropic consolidation stress of 100 kPa for the combination of sand with a) 5% fines content, and b) 15% fines content.

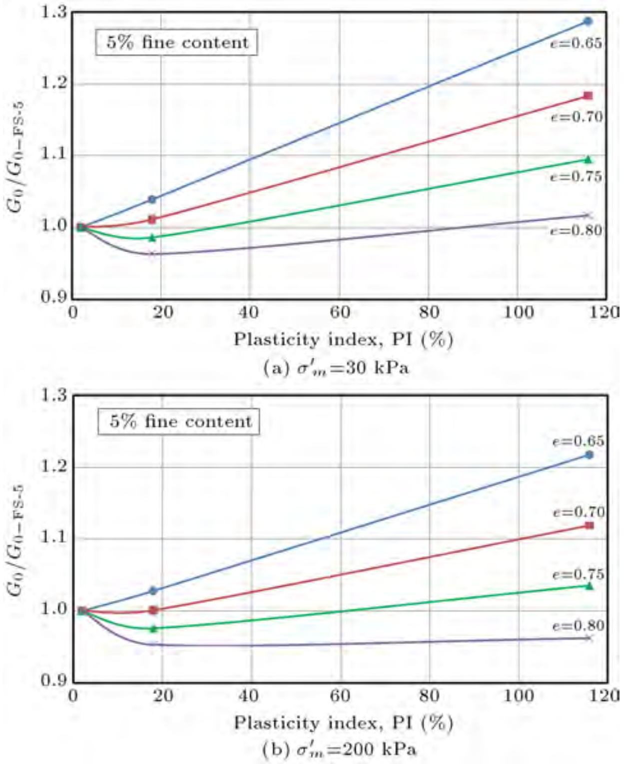

Figure 16. The G_0 value versus the plastic index of the fine part for 5% fines content at an isotropic consolidation stress of a) 30 kPa, and b) 200 kPa.

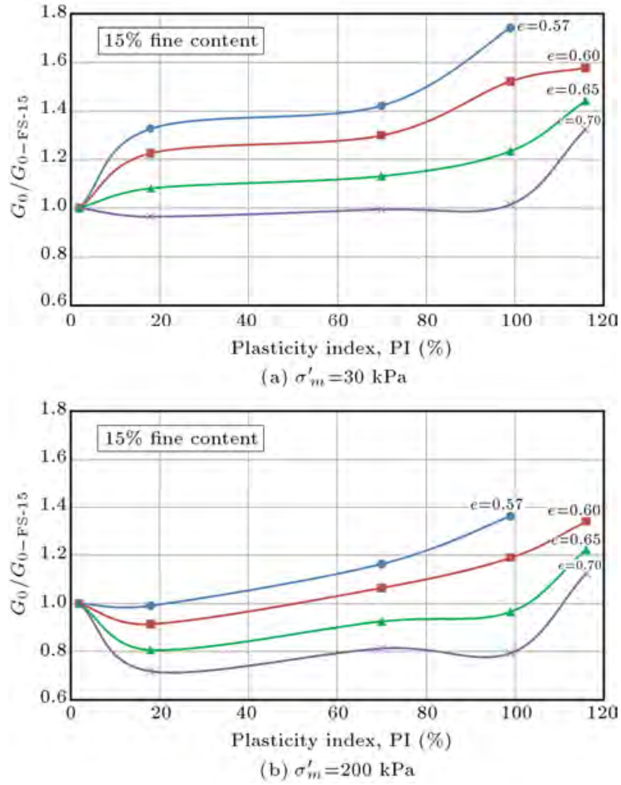

Figure 17. The G_0 value versus the plastic index of the fine part for 15% fines content at an isotropic consolidation stress of a) 30 kPa, and b) 200 kPa.

plasticity, and this dependency increases by increasing the fines content.

Two types of Plasticity Index (PI) can be used as a measure of plasticity for sand-fine mixtures: PI of the mixture (which is determined for portion of a soil that passes the 425-μm sieve) and PI of the fine part (which is determined for portion of a soil that passes the #200 sieve). If the PI of mixture is desired, only the combination of sand and 15% Bentonite (FB-15) have a PI of 7% and other tested materials should be considered non-plastic. It is therefore more convenient to use the PI of fine part as a measure of plasticity for sand-fine mixtures. The G_0 of sand-fines mixture normalized to G_0 of sand-silt mixture versus the plastic index of the fine part, separately for 5 and 15% fines content are drawn in Figures 16 and 17, respectively, at an isotropic consolidation stress of 30 and 200 kPa for different void ratios. As it can be seen, regardless of the fine percentage, at low void ratios (high density) G_0 increases with an increase in the plasticity of fine particles, but at high void ratios (low density) G_0 first decreases with an increase in the plasticity index and then increases with further increase in plasticity index. The amount of initial reduction of G_0 increases by increasing either the isotropic consolidation stress or the void ratio. Also, at higher confining stresses, G_0 initially reduces in the greater ranges of void ratio, because of increasing the PI value. This phenomenon can be interpreted as follows: At high void ratio, connections between fine and coarse particles are not developed effectively for low-plastic fines (Kaolin clay), since lubricating properties of clay particles outweigh the adhesion properties and therefore load does not transmit effectively at very small strains. By increasing plasticity or decreasing the void ratio, the adhesion properties overcome the lubrication properties and thus better contacts are developed between coarse and fine particles and so shear waves are transferred effectively.

By comparing Figures 16 and 17, it is clear that the effect of fines plasticity increases by increasing the fines content, so that in the range of void ratios and confining stresses tested in this study, for combination of sand with 5 and 15% fines content, the fines type could alter small-strain shear modulus less than 30% and up to 70%, respectively.

6. Conclusions

A comprehensive series of bender elements tests were performed on saturated isotropically consolidated samples of uniform clean sand and sand containing different amount of highly-plastic, medium-plastic, low-plastic or non-plastic (silt) fines. SEM imaging was also used to study the fabric of specimens of sands with fines. It was observed that:

- Empirical relations proposed by Hardin and Richart [3] and Jamiolkowski et al. [29] have high accuracy and are applicable for clean sand, silty sand, clayey sand, sandy silt and silt.
- Regardless of the fines type, increasing the fines content up to 15%, at a constant void ratio, decreases the G_0 value. This reduction is also continued if the non-plastic fines increase to 25%. But, as the void ratio ranges of tests were different for tested soils, it is difficult to conclude the same trend for higher fines contents. However, increasing the fines content from 25% to 35% and also from 35% to 50% will result in a decrease in G_0 at a constant void ratio. Increasing the fines content from 50% to 75%, G_0 values increase slightly. Therefore, it can be concluded that there is a threshold value for fines content beyond which higher G_0 values are anticipated. Threshold fines content for mixture of sand and silt tested is around 50% in this study. Obviously, threshold fines content depends on the characteristics of the base sand as well as the fines particles. For the tested materials in this study, at a given void ratio, the G_0 value for pure sand is about two times the G_0 value for silty materials.
- By adding a small amount of non-plastic fines (e.g. 3% and 5%) to sand at low void ratios, G_0 is significantly reduced, while this reduction is lower at high void ratios. The fabrics for silty sand with high percentage of silt (lower than threshold fines content) or low void ratio are floating, while silty sands with low percentage of non-plastic fines or silty sands with high void ratio have non-floating fabrics.
- Unlike the non-plastic fines, the rate of sand G_0 reduction due to adding highly-plastic fines is almost identical at different void ratios. This is because, very small size and high cohesion of plastic fine particles result in a fine layer surrounding the coarse particles independent of fines content or void ratio.
- If skeleton void ratio or equivalent granular void ratio is to be considered as density parameter, then for silty sand with less than 15% fines content, G_0 remains almost constant at a constant density parameter, especially at high skeleton or equivalent granular void ratios. However, with further increasing the fines, G_0 increases. The skeleton void ratio and equivalent granular void ratio are suitable density parameters for silty sands with low fines content (e.g. FC$\leq$15%). But these parameters are not suitable for silty sands with high fines content, sandy silts, or clayey sands.
- G_0 values depend on the fines type. For sand-fine mixtures, at constant void ratio, increasing the PI value of fine part may increase or decrease the G_0 value, depending on effective stress and void ratio. The effect of plasticity is reduced by increasing the effective confining stress, increasing the void ratio or decreasing the fines content.

Nomenclature

b	Active fraction of fines in force structure
C_g, a_g, n_g, e_g	Intrinsic soil parameters in the small-strain shear modulus evaluation from e and σ'_m
C_u	Coefficient of uniformity
D_{50}	Mean grain size
D_r	Relative density
e	Void ratio
e^*	Equivalent granular void ratio
$e_{\max}$	Maximum void ratio
$e_{\min}$	Minimum void ratio
e_s	Skeleton void ratio
FC	Ratio of dry weight of fines to the total dry weight of solids
G	Shear modulus
G_0	Small-strain shear modulus
G_s	Specific gravity of solids
K_0	Coefficient of lateral earth pressure at rest
L	Tip-to-tip distance of bender elements
LL	Liquid limit
P_A	Reference stress (=100 kPa)
PI	Plasticity index
R^2	Correlation coefficient
t	Travel time of the wave in bender element tests
V_s	Shear wave velocity
ρ	Total density
σ'_m	Mean effective stress
σ'_v	Vertical effective stress

References

1. Shirley, D.J. and Hampton, L.D. "Shear-wave measurements in laboratory sediments", *J. Acoust. Soc. Am.*, **63**(2), pp. 607-613 (1977).
2. Dyvik, R. and Madshus, C. "Laboratory measurement of $G_{\max}$ using bender elements", *Advances in the Art of Testing Soils Under Cyclic Conditions, ASCE*, New York, pp. 186-196 (1985).
3. Hardin, B.O. and Richart, F.E.J. "Elastic wavevelocities in granular soils", *J. Soil Mech. Found. Div.*, **89**(1), pp. 33-65 (1963).

4. Chung, R.M., Yo Kel, F.Y. and Drenevich, V.P. "Evaluation of dynamic properties of sands by resonant column testing", *Geotech. Testing J.*, **7**(2), pp. 60-69 (1984).

5. Bolton, M.D. "The strength and dilatancy of sands", *Géotechnique*, London, **36**(1), pp. 65-78 (1986).

6. Lo Presti, D.C.F. "Mechanical behavior of Ticino sand from resonant column tests", PhD Thesis, Politecnico di Torino, Turin, Italy (1987).

7. Zhou, Y.G. and Chen, Y.M. "Influence of seismic cyclic loading history on small-strain shear modulus of saturated sands", *Soil Dyn. Earthquake Eng.*, **25**(5), pp. 341-353 (2005).

8. Youn, J.U., Choo, Y.W. and Kim, D.S. "Measurement of small-strain shear modulus $G_{\max}$ of dry and saturated sands by bender element, resonant column, and torsional shear tests", *Can. Geotech. J.*, **45**(10), pp. 1426-1438 (2008).

9. Wichtmann, T. and Triantafyllidis, T. "Influence of the grain-size distribution curve of quartz sand on the small-strain shear modulus $G_{\max}$", *J. Geotech. Geoenviron. Eng.*, **135**(10), pp. 1404-1418 (2009).

10. Wichtmann, T., Navarette Hernandez, M., Martinez, R., Duran Graeff, F., Giolo, E. and Triantafyllidis, Th. "Estimation of the small-strain stiffness of granular soils taking into account the grain size distribution curve", *Fifth International Conference on Earthquake Geotechnical Engineering*, Santiago, Chile (2011).

11. Hardin, B.O. and Black, W.L. "Vibration modulus of normally consolidated clay", *J. Soil Mech. and Found. Div.*, **94**(2), pp. 353-369 (1968).

12. Hardin, B.O. "The nature of stress strain behavior for soils", *Proc. ASCE Geotech. Engrg. Div. Specialty Conf. on Earthquake Engineering and Soil Dynamics*, **1**, pp. 3-90 (1978).

13. Jamiolkowski, M., Lancellotta, R. and Lo Presti, D.C.F. "Remarks on the stiffness at small-strains of six Italian clays", *Pre-Failure Behavior of Geomaterials*, S. Shibuya, T. Mitachi, and S. Miura, Eds., **2**, Balkema, Rotterdam, The Netherlands, pp. 817-854 (1995).

14. Shibuya, S., Hwang, S.C. and Mitachi, T. "Elastic shear modulus of soft clays from shear wave velocity measurement", *Géotechnique*, **47**(3), pp. 593-601 (1997).

15. Jovicic, V. and Coop, M.R. "The measurement of stiffness anisotropy in clays with bender element tests in the triaxial apparatus", *Geotech. Test. J.*, **21**(1), pp. 3-10 (1998).

16. Santagata, M.C., Germaine, J.T. and Ladd, C.C. "Initial stiffness of K_0-normally consolidated Boston blue clay measured in the triaxial apparatus", *Pre-Failure Deformation Characteristics of Geomaterials*,M. Jamiolkowski, R. Lancellotta, and D. Lo Presti, Eds., **1**, Balkema, Rotterdam, The Netherlands, pp. 27-34 (1999).

17. Santagata, M., Germaine, J.T. and Ladd, C.C. "Factors affecting the initial stiffness of cohesive soils", *J. Geotech. Geoenviron. Eng.*, **131**(4), pp. 430-441 (2005).

18. Santagata, M., Germaine, J. and Ladd, C. "Small-strain nonlinearity of normally consolidated clay", *J. Geotech. Geoenviron. Eng.*, **133**(1), pp. 72-82 (2007).

19. Cho, W. and Finno, R.J. "Stress-strain responses of block samples of compressible Chicago glacial clays", *J. Geotech. Geoenviron. Eng.*, **136**(1), pp. 178-188 (2010).

20. Liu, N. and Mitchell, J.K. "Influence of non-plastic fines on shear wave velocity-based assessment of liquefaction", *J. Geotech. Geoenviron. Eng.*, **132**(8), pp. 1091-1097 (2006).

21. Iwasaki, T. and Tatsuoka, F. "Effects of grain size and grading on dynamic shear moduli of sands", *Soils Found.*, **17**(3), pp. 19-35 (1977).

22. Randolph, M.F., Dolwin, J. and Beck, R. "Design of driven piles in sand", *Géotechnique*, **44**(3), pp. 427-448 (1994).

23. Salgado, R., Bandini, P. and Karim, A. "Shear strength and stiffness of silty sand", *J. Geotech. Geoenviron. Eng.*, **126**(5), pp. 451-462 (2000).

24. Huang, Y.T., Huang, A.B., Kuo, Y.C. and Tsai, M.D. "A laboratory study on the undrained strength of a silty sand from central western Taiwan", *Soil Dyn. Earthquake Eng.*, **24**, pp. 733-743 (2004).

25. Dobry, R. and Vucetic, M. "Dynamic properties and seismic response of soft clay deposits", *Proceedings, International Symposium on Geotechnical Engineering of Soft Soils*, Mexico City, **2**, pp. 51-87 (1987).

26. Zen, K., Umehara, Y. and Hamada, K. "Laboratory tests and in situ seismic survey on vibratory shear modulus of clayey soils with various plasticities", *Proc., 5th Japan Earthquake Engineering Symp.*, Architectural Institute of Japan, Tokyo, Japan, pp. 721-728 (1978).

27. Wang, G.X. and Kuwano, J. "Modeling of strain dependency of shear modulus and damping of clayey sand", *Soil Dyn. Earthquake Eng.*, **18**, pp. 463-471 (1999).

28. Carraro, J.A.H., Prezzi, M. and Salgado, R. "Shear strength and stiffness of sands containing plastic or nonplastic fines", *J. Geotech. Geoenvir. Eng.*, **129**(11), pp. 1167-1178 (2009).

29. Jamiolkowski, M., Leroueil, S. and Lo Presti, D.C.F. "Theme lecture: Design parameters from theory to practice", *Proc. Geo-Coast '91*, Yokohama, **2**, pp. 877-917 (1991).

30. Ishihara, K. "Liquefaction and flow failureduring earthquakes", *Géotechnique*, **43**(3), pp. 351-415 (1993).

31. Ladd, R.S. "Preparing test specimens using undercompaction",*Geotech. Test. J.*, **1**(1), pp. 16-23 (1978).

32. Bahadori, H., Ghalandarzadeh, A. and Towhata, I. "Effect of non plastic silt on the anisotropic behavior of sand", *Soils Found.*, **48**(4), pp. 531-545 (2008).

33. Lee, J.S. and Santamarina, J.C. "Bender elements: Performance and signal interpretation", *J. of Geotech. Geoenviron. Eng.*, **131**(9), pp. 1063-1070 (2005).

34. Kumar, J. and Madhusudhan, B.N. "A note on the measurement of travel times using bender and extender elements", *Soil Dyn. Earthquake Eng.*, **30**(7), pp. 630-634 (2010).

35. Sladen, J.A. and Handford, G. "A potential systematic error in laboratory testing of very loose sands", *Can. Geotech. J.*, **24**(3), pp. 462-466 (1987).

36. Pitman, T.D., Robertson, P.K. and Sego, D.C. "Influence of fines on the collapse of loose sands", *Can. Geotech. J.*, **31**, pp. 728-739 (1994).

37. Yamamuro, J.A. and Covert, K.M. "Monotonic and cyclic liquefaction of very loose sand with high silt content", *J. Geotech. Geoenviron. Eng.*, **127**(4), pp. 314-324 (2001).

38. Derakhshandi, M., Rathje, E.M., Hazirbaba, K. and Mirhosseini, S.M. "The effect of plastic fines on the pore pressure generation characteristics of saturated sands", *Soil Dyn. Earthquake Eng.*, **28**(5), pp. 376-386 (2008).

39. Thevanayagam, S., Shenthan, T., Mohan, S. and Liang, J. "Undrained fragility of clean sands, silty sands, and sandy silts", *J. Geotech. Geoenviron. Eng.*, **128**(10), pp. 849-859 (2002).

40. Rahman, M.M., Lo, S.R. and Gnanendran, C.T. "On equivalent granular void ratio and steady state behaviour of loose sand with fines", *Can. Geotech. J.*, **45**(10), pp. 1439-1455 (2008).

41. Georgiannou, V.N., Burland, J.B. and Hight, D.W. "The undrained behaviour of clayey sands in triaxial compression and extension", *Géotechnique*, **40**(3), pp. 431-449 (1990).

42. Thevanayagam, S. "Effect of fines and confining stress on undrained shear strength of silty sands", *J. of Geotech. Geoenviron. Eng.*, **124**(6), pp. 479-491 (1998).

43. Thevanayagam, S. "Liquefaction potential and undrained fragility of silty soils", In *Proc. 12th World Conf. Earthquake Engineering.*, Edited by R. Park. Auckland, New Zealand. New Zealand Society of Earthquake Engineering, Paper #2383 (2000).

44. Thevanayagam, S. "Role of intergranular contacts on the mechanisms causing liquefaction and slope failures in silty sands", In *Annual Project Summary Report. US Geological Survey*, Department of Interior, Washington D.C. (2001).

45. Ni, Q., Tan, T.S., Dasari, G.R. and Hight, D.W. "Contribution of fines to the compressive strength of mixed soils", *Géotechnique*, **54**(9), pp. 561-569 (2004).

46. Yang, S.L., Sandven, R. and Grande, L. "Instability of sand-silt mixtures", *Soil Dyn. Earthquake Eng.*, **26**(2-4), pp. 183-190 (2006).

Biographies

Nima Akbari Paydar received his PhD and MS degrees in Geotechnical Engineering from Sharif University of Technology in 2014 and from Tehran University in 2006, respectively. He is currently an Assistance Professor in the Civil Engineering Department of Tabriz University. Dr. Akbari Paydar's primary research interests include: soil dynamics, experimental geotechnics, geotechnical equipment construction, dam engineering, and instrumentation of geotechnical structures. He has been involved in many dam projects in the recent eight years as Senior Geotechnical Engineer.

Mohammad Mehdi Ahmadi received his PhD degree in Geotechnical Engineering from the Department of Civil Engineering at the University of British Columbia, Vancouver, Canada in 2000. He is currently an Associate Professor of Geotechnical Engineering in the Civil Engineering Department of Sharif University of Technology. Dr. Ahmadi's research interests cover a variety of subjects, including site characterization for earthquake design, in-situ testing of soils, numerical modeling, static and dynamic soil-structure interaction, unsaturated soil, case histories, and foundations for offshore structures.